Feeder-Link Outage Prediction Algorithms for SDN-based High-Throughput Satellite Systems

Maurizio Mongelli [§], Tomaso De Cola [*], Marco Cello [#], Mario Marchese [†], Franco Davoli [†]
[§] National Research Council, Genoa, Italy
maurizio.mongelli@ieiit.cnr.it
[#] Nokia Bell Labs, Dublin, Ireland
marco.cello@nokia.com
[*] German Aerospace Center (DLR), Oberpfaffenhofen, Germany
tomaso.decola@dlr.de
[†] University of Genoa, Genoa, Italy
mario.marchese@unige.it, franco.davoli@unige.it

***Abstract*—The design of High Throughput Satellite (HTS) systems builds on the concept of Smart Gateway Diversity (SGD) to exploit the spatial diversity of gateways in case of feeder link outage, occurring because of atmospheric impairments introduced in Extremely High Frequency (EHF) frequency bands. The gateway handover procedure requires precise prediction algorithms and coordination among different network elements. This paper presents novel outage prediction algorithms based on machine learning concepts, integrated in the framework of SDN architectures, to efficiently orchestrate the gateway handover operations. Simulation campaigns prove the validity of the proposed concept and shed light on the potentials of the SDN architecture in future HTS systems.**

I. Introduction

The increasing demand for high-throughput services (e.g., UHDTV) and anywhere-anytime Internet connectivity have pushed satellite industry and operators towards the design and development of a new class of High Throughput Satellite (HTS) systems, exploiting Extremely High Frequency (EHF) frequency bands (>30 GHz) in the feeder link. This concept allows dramatically increasing the overall aggregate satellite capacity (terabit/s),provided that the severe atmospheric impairments introduced in these frequency bands are properly counteracted by sophisticated gateway diversity concepts (e.g., Smart Gateway Diversity (SGD)).

In this regard, the scientific community has thoroughly investigated the propagation aspects and proposed different SGD architectures [1], mostly focusing on capacity-achieving concepts. More recently, some attention has been also given to gateway handover techniques relying on the application of network coding and new channel prediction algorithms [2]. In spite of the effort dedicated so far to these aspects, there is no full understanding of the network architecture implications when satellite and terrestrial networks are integrated to implement the SGD concept. The EU-funded BATS project (http://www.batsproject.eu/) proposed some preliminary solutions, consisting in the use of dedicated links to interconnect gateways or to rely on the existing terrestrial network infrastructure. However, no specific analysis of the coordination between terrestrial and satellite networked nodes has been carried out. On the other hand, the effectiveness of the gateway handover procedure is very much influenced by the accuracy of the employed channel outage prediction algorithm, whose foundation is given in ITU-R recommendations [3].

According to the aforementioned research gaps, the paper proposes novel channel prediction algorithms based on machine-learning concepts, which are used to optimize the performance of the gateway handover procedure. On the other hand, the coordination of network nodes, as supporting efficient handover operations, is framed in the context of Software Defined Networking (SDN) architectures, whose recent preliminary studies showed promising potentials also for applicability to satellite networks [4].

The remainder of this paper is structured as follows. Section II introduces the reference system, putting emphasis on the main features of the SDN-based architecture with respect to the gateway handover procedures as well as outage link prediction schemes. Section III formulates the outage prediction problem and proposes machine-learning based solutions. The performance assessment is reported in Section IV, where indications about the most promising techniques are also provided. Finally, Section V draws conclusions and summarizes open research points, which will be addressed in future extensions of this work.

II. Reference System

A. Satellite Scenario

This paper considers a star multi-beam multi-gateway satellite network and focuses on the feeder up-link, implementing the DVB-S2 technology [5]. The overall satellite network is controlled by a set of Network Control Centres (NCCs), whose functions can be co-located in the gateways. The feeder-link established between a gateway and the satellite, corresponding to the forward up-link and the return down-link, operates in the Q/V frequency bands (33-50 and 50-75 GHz, respectively). On the other hand, the user link established between satellite

978-1-4799-6664-6/16/$31.00 ©2016 IEEE

terminals and satellite, corresponding to the forward down-link and return up-link, operates in the Ka frequency band (27-40 GHz). The use of EHF frequency bands for data communications, however, poses formidable challenges in terms of propagation impairments (especially because of rain fading), which may cause gateway feeder-link outage events, whereby gateway handover procedures are necessary. Further to this, achieving high service availability figures (>99.5%) requires the implementation of the smart gateway diversity architecture, so that back-up gateways or spare capacity are made available in order to serve the additional data traffic load resulting from gateway handover events.

In this context, it is immediate to see that 1) network architectural implications and 2) link outage prediction are of paramount importance to properly design the overall network. As to the former, re-routing mechanisms during the handover procedure have to be carefully designed, properly supported by the decision-making and coordination schemes necessary to select and re-configure the gateways towards which the re-routed traffic should be forwarded. As to the latter, the detection of a forthcoming outage event, which is based on the "strength" of the beacon signal received from the satellite, must be performed so as to avoid delayed handover operations, which might result in intolerably high packet loss rates, as argued in [2]. The two aforementioned points are further elaborated in the next two sections.

B. SDN-based Architecture

The need for network nodes' coordination and re-configuration, as stated in the previous section, calls for new networking functions that can be conveniently offered by the SDN concept. SDN is revolutionizing the networking industry by enabling programmability, easier management and faster innovation [6], [7]. These benefits are made possible by its centralized control plane architecture, which allows the network to be programmed by the application and controlled from one central entity.

The SDN architecture is composed of both switches/routers[1] and a central controller (SDN controller). SDN-enabled devices process and deliver packets according to rules stored in the flow table (forwarding state), whereas the SDN controller configures the forwarding state of each switch using a standard protocol: OpenFlow (OF) [7].

Handover procedures in a HTS system can be efficiently implemented using the real-time capabilities of SDN and in particular the re-routing procedures of a set of flows from a gateway experiencing link outage to another one.

Specifically, we consider the satellite networks scenario depicted in Figure 1, in which 3 gateways (GW1, GW2, GW3) are connected to the satellite 'SAT' and to the upstream SDN-enabled switches (S1, S2, S3), respectively. S1, S2, S3 are controlled by an SDN Controller using OpenFlow, whereas GW1, GW2, GW3 and NCC1, NCC2, NCC3 are managed by the NCC/GW Manager through dedicated control protocols.

[1]In the following we will use the terms: SDN devices, OpenFlow devices, OpenFlow switches, interchangeably.

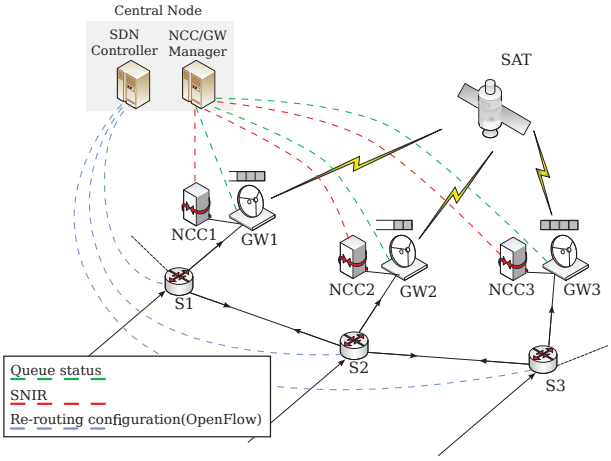

Fig. 1. Smart Gateway Diversity Scenario.

NCCs periodically send to information about measured SINR of controlled feeder links NCC/GW Manager, while GWs send information about the occupation of the corresponding queue.

The Central Node is the joint entity composed of the NCC/GW Manager and the SDN Controller and represents the intelligence of the entire network. On the one hand, it receives information about physical parameters of the link (computation of SINR and queue occupation) and computes the probability of feeder link outage. On the other hand, it decides which flows, traversing the gateway experiencing future outage, should be re-routed to alternative gateways.

Figure 2 shows the block diagram representation of the Central Node. Prediction of link outage and estimation of congestion events occurring at GWs can be implemented as functions running on top of the SDN Controller (northbound applications). In turn, the SDN Controller exposes its functionalities to the northbound applications (flows map, routing map). Finally, the rerouting Engine is responsible for identifying the traffic flows that need to be migrated and informs the Routing Manager/Flows Rule Generator, creating the OF rules for S1, S2, S3.

It can be noticed that the architecture proposed in this paper follows the design principles also explored in [4]. However, differently from [4], the two managers (i.e., SDN Controller and NCC/GW Manager) are implemented as two separated entities that are joined through proper control primitives (the dotted lines in Figure 2). Further to this, [4] does not thoroughly explain the functions carried out by the SDN Controller, whereas our proposal elaborates feeder-link outage prediction algorithms that should be performed by the Central Node. It can be also noticed that the availability of information about outage events and gateway queue occupation can be exploited by the SDN controllers also to implement more efficient Quality of Service (QoS) management solutions, which is however beyond the scope of this paper.

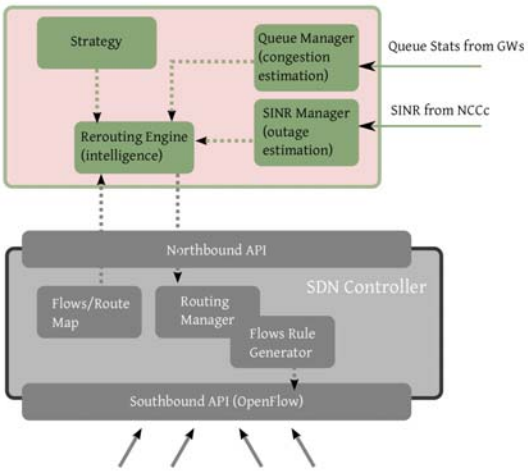

Fig. 2. Block Diagram of the Central Node.

C. Prediction of Feeder Link Outage Events

The prediction of forthcoming feeder link outage events is a key function to properly and efficiently perform handover operations. Link outage events are typically detected on the basis of the SNR figures computed according to the received power of satellite beacons. Accurate estimation of outage events timing is especially relevant in the reference application domains (e.g., HTS systems operating in EHF), where loose forecast of such events can give rise to either feeder link capacity waste or excessive packet loss. The former may occur in case of conservative estimation of the time instant, in which the feeder link will be no longer available, resulting in unnecessary anticipation of handover operations. On the other hand, the latter can happen when a network operator attempts to take advantage of the satellite capacity as much as possible, hence excessively delaying the handover execution and eventually resulting in information loss. From this standpoint it is immediate to grasp the importance of accurate outage estimation.

Starting from the early 90's, a significant literature exists on SNR prediction over satellite channels, in particular in the Ka band context. [8] exploits linear regression to anticipate an outage event of 2 s. [9] shows how a neural network may achieve better performance than traditional statistical and autoregressive moving average (ARMA) methods. Studies on non-linear models have received interest more recently, see, e.g., [10]. A control-theoretic perspective is provided to the problem in [11], by updating system statistics from real data. [11] discusses also how the relation between prediction and the linear trend of data may be hardly investigated. In [12], ARMA is used with closed-form expressions of the performance measures (outage probability and prediction error) with an anticipation time of 10 s. In the Q/V band, recent studies [13] address the derivation of analytic expressions of prediction and outage probabilities. The sensitivity to rain and the high rate of the Q/V band lead to further investigations of prediction methods with large anticipation of outage events. The largest part of the approaches in the literature exploits either function regression (also used here as a performance comparison) or probabilistic methods.

D. Paper Contribution

The main contribution of this paper is to develop a feeder link outage prediction algorithm operated without any a-priori assumption on the probability distribution of the SNR, taking advantage of supervised learning concepts [14]. The intuition behind the approach is the formulation of the SNR prediction as a classification problem, where the results of SNR pre-processing (i.e., filtering by first order regression) is given as input to the classifier. Regression techniques have been used as performance benchmarks to validate the proposed concept.

III. Prediction Problem

A. Problem Statement

The problem consists of predicting whether the SNR will be below a given threshold at a given time in the future. The threshold is typically associated to a channel outage event. The prediction is done on the basis of past SNR samples, acquired over a given observation horizon. Let s be the SNR signal discretized over time; $s(t)$ denotes the sample at time t. A new prediction is provided at each discrete time $t = 1, 2, ...,$ on the basis of the information vector $\boldsymbol{I}(t) = [\ s(t-T+1), ..., s(t-j), ..., s(t)\ ]$, T being the size of the observation window over the past and $j = 0, .., T-1$. The i^{th} component of the information vector $\boldsymbol{I}(t)$ will be henceforth referred to as $s_j(t) = s(t-j)$. The prediction is with respect to time $(t+t_d)$, t_d being the time lag into the future. The outage threshold is denoted by γ_{th}. Let $f(\boldsymbol{I}(\cdot), \cdot)$ a generic prediction function. An outage is foreseen at time t if $f(\boldsymbol{I}(t), t+t_d) > \gamma_{th}$.

B. Proposed Prediction Algorithms

The proposed prediction algorithms exploit regression approximation of the reference function $f(\boldsymbol{I}(\cdot), \cdot)$, of which only a set of samples is available.

1) Linear Regression: Linear regression (LR) is performed at each time t on the samples collected in $\boldsymbol{I}(t)$. The coefficients for the slope $m(t)$ and the intercept $q(t)$ in the linear regression are computed according to a least-squares approach as follows:

$$m(t) = \frac{T \cdot \sum_{j=0}^{T-1} j \cdot s_j(t) - \sum_{j=0}^{T-1} j \cdot \sum_{j=0}^{T-1} s_j(t)}{T \cdot \sum_{j=0}^{T-1} j^2 - (\sum_{j=0}^{T-1} j)^2} \quad (1)$$

$$q(t) = \frac{\sum_{j=0}^{T-1} s_j(t) - m(t) \cdot \sum_{j=0}^{T-1} j}{T} \quad (2)$$

The parameters m and q are derived with a small computational cost independent of T, because the number of operations at every new sample is always the same. Once the parameters have been updated at time t, the prediction by linear regression, $\hat{s}_{reg}$, at any time t' in the future ($t' > t$) is $\hat{s}_{reg}(t') = m(t) \cdot t' + q(t)$. The corresponding prediction is derived by verifying whether $\hat{s}_{reg}(t+t_d) \leq \gamma_{th}$ (no outage is predicted) or not (an outage is predicted). No datasets

are needed on historical SNR data, because a new $\hat{s}_{reg}$ is inferred at any time according to the last update of the linear parameters. The technique automatically adapts to the trend currently present in the SNR signal.

2) Neural Network: A neural network (NN) is used to track the non-linearity of the SNR evolution over time. A dataset is defined on the basis of the information vector $\boldsymbol{I}(t)$ over k observation windows as follows: $\Psi_{NN} = \{(\boldsymbol{I}^k, s_k^*), k = 0, ..., K-1\}$, where dependency on time t has been dropped to simplify the notation and s_k^* is the signal prediction target at $t + t_d$, i.e. $s(t + t_d)$. Hence, the Ψ_{NN} dataset maps each $\boldsymbol{I}^k$ into the corresponding signal at time $(t + t_d)$. A neural network is defined with the same input $\boldsymbol{I}^k(\cdot)$ and with weights $\boldsymbol{\varepsilon}$: $\hat{s}_{NN}(I^k(\cdot), \boldsymbol{\varepsilon})$. A neural training problem is then derived from the Ψ_{NN} dataset. The NN training consists of finding the weights assignment $\boldsymbol{\varepsilon}^*$ so that:

$$\boldsymbol{\varepsilon}^* = \arg\min_{\boldsymbol{\varepsilon}} J(\boldsymbol{\varepsilon}); J(\boldsymbol{\varepsilon}) = \sum_{k=0}^{K-1} [s_k^* - \hat{s}_{NN}(\boldsymbol{I}^k, \boldsymbol{\varepsilon})]^2. \quad (3)$$

Problem (3) consists of a regular neural regression scheme that tunes the output of the NN in order to learn the $\{\boldsymbol{I}\}$ mapping collected in Ψ_{NN} through the function $\hat{s}_{NN}$. Operatively, as similarly discussed for LR, once (3) is solved, the resulting NN may be used to infer new values of s_k^* according to new values of $\boldsymbol{I}$. The prediction is performed as in the previous subsection by replacing $\hat{s}_{reg}$ with $\hat{s}_{NN}$. In practice, a re-training may be started each time a new dataset of SNR is acquired. This helps follow SNR fluctuations and avoids using the NN with historical information which may be too old to drive the right prediction at the current time.

C. Classification

1) Rationale: The prediction function $f(\boldsymbol{I}(\cdot), \cdot)$ (section III-A) is now investigated by posing the problem under a classification setting. The amount of information needed to solve a classification problem is considerably lower than that required in a regression problem [15].

A classification problem is formulated as follows. Let $\omega = 0$ or 1 denote the under- or over-threshold events, namely, $s(t + t_d) \leq \gamma_{th}$ or otherwise, respectively. Let $\Psi = \{(\boldsymbol{I}^k, \omega^k), k = 0, ..., K-1\}$ be a dataset corresponding to the collection of the SNR in absence and in the presence of outage events. More specifically, $\boldsymbol{I}^k$ contains no-outage events if $\omega^k = 0$, i.e. $s(t + t_d) \leq \gamma_{th}$, whereas it contains outage events if $\omega^k = 1$. The same conditions hold if one-step shift over the SNR trace is applied to consider $\boldsymbol{I}^{k+1}$. The collection of points in Ψ are derived by iterating over the available SNR trace. The classification problem consists of finding the best boundary function $g(\cdot)$ separating the $\boldsymbol{I}^k$ points in Ψ, according to the two classes $\omega = 0$ or $\omega = 1$[2].

Several algorithms are available to find $g(\cdot)$ according to the supervised learning literature [14]. As reported in the results, if the feature vector lies in (or may be projected into) a bi-dimensional (or three-dimensional) space, Ψ may be easily visualized to give a first insight into the difficulty of the problem (i.e., how much the available samples of the feature vector are separable with respect to the two classes). Once $g(\cdot)$ is available, it may be used in the following way. The current SNR signal is inspected by building a new vector $\boldsymbol{I}'$ on the basis of the last T samples; the corresponding prediction is derived by comparing $\boldsymbol{I}'$ with $g(\cdot)$.

2) Bayes: One of the most traditional and simplest classifiers is used to find $g(\cdot)$ from Ψ: the so-called Bayes classifier (see, e.g., chapter I of [14], also known as 'normal-based discriminant analysis').

As a first step, the original $\boldsymbol{I}^k$ data are mapped into another space $\boldsymbol{I}_r$ corresponding to the parameters of linear regression: $\boldsymbol{I}_r^k = \{(m^k, q^k), k = 0, ..., T-1\}$, m^k, q^k being the parameters originated from $\boldsymbol{I}^k$ as explained in section III-B1. This step helps map the current linear trend of SNR into the two classes. Two multivariate normal probability distributions, $p_1(\boldsymbol{I}_r|\omega = 1)$ and $p_0(\boldsymbol{I}_r|\omega = 0)$, are built from the training set (e.g., a subset of Ψ) under the 'maximum likelihood parameter estimation' paradigm, by data corresponding to the outage class when building the first normal distribution and data corresponding to non-outage events for the second one [16]. A new feature vector $\boldsymbol{I}_r^h$ is assigned to the outage class if $p_1(\boldsymbol{I}_r^h|\omega = 1) > p_0(\boldsymbol{I}_r^h|\omega = 0)$ (by assuming equal a-priori probabilities of the two classes). Since a pooled covariance matrix estimation is used when building the two probability distributions, the obtained classification rule draws linear boundaries between regions of space allocated to 'outage' and 'no outage' groups of data. The $g(\cdot)$ function thus becomes a linear boundary and acts as follows. Given a new sample $\boldsymbol{I}_r'$, *if* $((K - 1 + L_1 \cdot q' + L_2 \cdot m') \leq 0\ )$ ω'=1, *else* ω'=0; $K,\ L_1,\ L_2$ being the linear boundaries obtained by the equalization of the two probability distributions $p_1(\cdot|\omega = 1)$ and $p_0(\cdot|\omega = 0)$ [16].

The method assumes a Gaussian distribution of the features in each class. This is an approximation and may lead to a classification error, whose detrimental effect may be circumvented by using more complex classifiers, such as Support Vector Machines, neural networks or others. Even though the distribution of $\boldsymbol{I}_r$ samples graphically suggests that the Gaussian assumption does not hold for outage data (Fig. 5 further on) and that the best $g(\cdot)$ should assume a non-linear trajectory in the $\boldsymbol{I}_r$ space, the good results obtained here corroborate the reliability of the approach. Bayes is also preferable in terms of computational effort with respect to other classifiers.

IV. Results

A. Performance Measure

The performance metrics of interest are the *false positive* and *false negative rates* (FPR, FNR). The former is the measure of how many times an outage is predicted, but it does not happen in reality. The latter is analogously related to outages not correctly predicted.

[2]In this context, $\boldsymbol{I}$ is called the 'vector of features', the features being the samples s_k in $\boldsymbol{I}^k$.

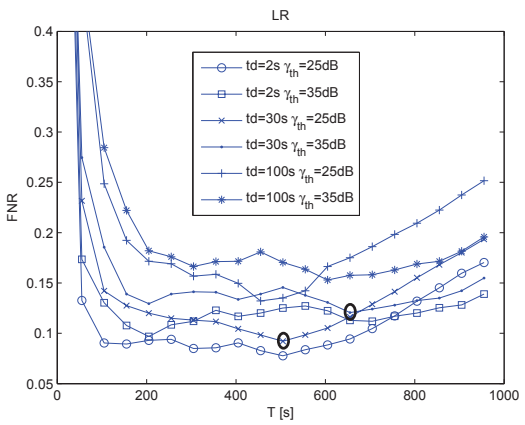

Fig. 3. Linear regression.

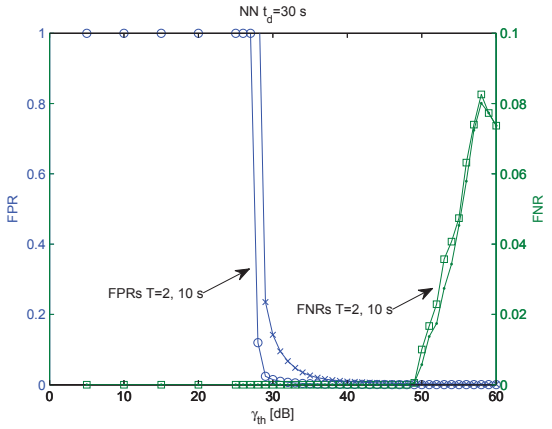

Fig. 4. Neural regression.

B. Simulation Scenario

The considered satellite network is composed of a number of gateways operating throughout Europe, connecting to a geostationary satellite with a communication link established at a central frequency of 50 GHz. The performance analysis is focused on the propagation impairments experienced by a satellite station, which was assumed as located in Weilheim (Germany). The computation of the overall signal attenuation (e.g., scintillation and rain fading) was done according to synthetic traces, recorded over 2 months period, with sampling time 1 s. On the basis of point-to-point link budget computations and use of ModCod thresholds (according to DVB-S2 specification), it was possible to map feeder link outage events to the cases where the overall attenuation was in the range $25 - 35$ dB, so as to take into account different link margins.

The training for NN and Bayes is done with respect to a portion of the trace with a significant portion of outage events (10^6 samples). The test is performed over the entire trace ($5.4 \cdot 10^6$ samples), which contains other outage events, not used for training. LR is directly tested over the entire trace. An IntelCore i7-3630QM@2.4GHz has been used with Matlab version R2014b.

C. Linear Regression

The performance of LR is considered in Fig. 3. Since FPRs are of the order of 10^{-3}, only the FNRs are depicted with respect to the T parameter. For each curve, there is always a global minimum (T^*). The minima are different for each curve. The centers of the two circles in the figure show the minima of the t_d=30 cases with $\gamma_{th} = 25$ and $\gamma_{th} = 35$ dB[3]. In general, the curves show a flat trend in the T=$[100, 600]$ range, apart from the cases with $t_d = 100$ s. With $t_d = 30$ s, T^* leads to FNRs around 0.1 with both thresholds. Both NN and Bayes experience better performance with large t_d.

D. Neural Regression

A neural network with 5 and 8 hidden neural units is used with $T = 2$ and 10 s, respectively, with hyperbolic tangent activation function. The training is done through the Levenberg-Marquardt algorithm [17]. The database driving the training phase is divided in 70% of samples for training and 15% for both validation and test. To avoid overfitting [4] , the minimum number of hidden neural units is empirically found in correspondence of the minimum J, defined in (3).

The time for training has been fixed to 8'; after that time, in both cases with $T = 2$ and 10 s, the cost has completed its steepest descent. Information vectors larger than T=10 s have not been explored to avoid computational burden and the difficulty of choosing the best setting in the number of neural units.

Fig. 4 shows the error rates by changing the threshold γ_{th} with $t_d = 30$ s. The case of $t_d = 60$ s is qualitatively very similar, apart from the differences reported in the following. The ranges of γ_{th} with zero error rates are in $[30, 50]$ and $[30, 40]$ dB with $t_d = 30$ and 60 s, respectively (the largest anticipation time, $t_d = 60$, clearly reduces the performance of the classifier). Outside these ranges, the error rates increase exponentially, thus limiting the applicability of NN. Increasing T from 2 to 10 s does not lead to a significantly better performance. The maximum value of FPR is 1, whereas those of FNR are 0.082 and 0.2 with $t_d = 30$ and 60 s, respectively.

E. Bayes

The inherent computational time for training is of the order of some seconds. Fig. 5 shows the linear separator of Bayes (dashed line) between the two classes under the following setting: $T = 30$ s, $t_d = 30$ s and $\gamma_{th} = 35$ dB. The figure helps appreciate how the samples are distributed among the two classes in the $\boldsymbol{I}_r$ space. The outage case experiences more oscillations of the feature vector.

Fig. 6 shows all the linear separators obtained with Bayes under all the combinations of: $T = \{5, 30, 60\}$ s; $t_d = \{30, 60\}$ s; $\gamma_{th} = \{25, 35\}$ dB. The performance can be summarized for all the combinations as follows. FPRs are

[3]Please note that here γ_{th} denotes the threshold on the channel attenuation, whereas in Section III-A it referred to the received SNR

[4]In neural training, overfitting may be avoided by increasing the number of hidden neural units while the learning error decreases. When such an error reaches a steady state, the minimum number of hidden neural units is found.

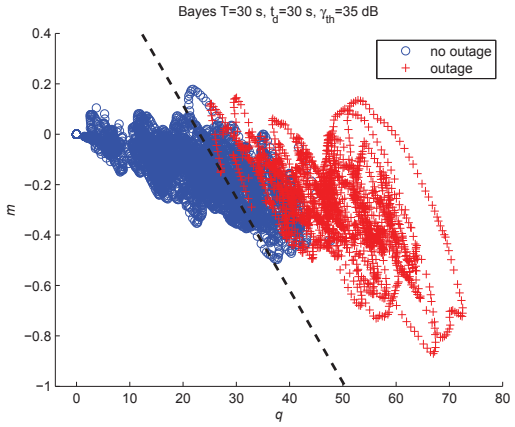

Fig. 5. Bayes classifier and samples of the $\boldsymbol{I}_r$ space.

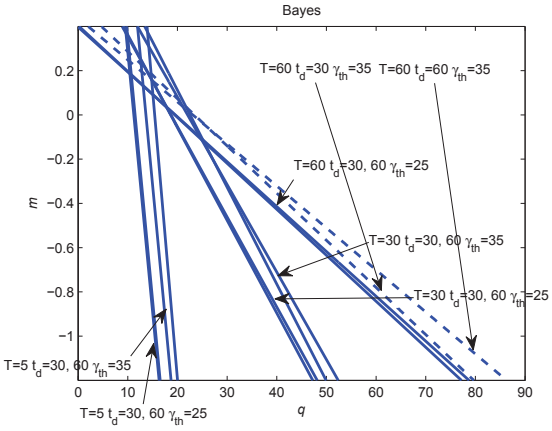

Fig. 6. Bayes classifiers under variable parameters.

always of the 10^{-3} order; FNRs are around $2 \cdot 10^{-2}$ with $\gamma_{th} = 25$ dB and $5 \cdot 10^{-3}$ with $\gamma_{th} = 35$ dB. The higher FNR with 25 dB is due to the fact that decreasing γ_{th} to 25 dB implies increasing the overlap of the classes. In other words, similar values of m and q are mapped on different classes more often than with $\gamma_{th} = 35$ dB, thus introducing more confusion into the classifier.

The following properties of the lines may be appreciated as well, by analyzing the figure in more details. Under equal values of T and γ_{th}, $t_d = 30$ and 60 lead to the same separator, apart from the case with $T = 60$ and γ_{th}=35, which shows two slightly different lines with $t_d = 30$ and 60 s (the two dashed lines in the figure). Moreover, the groups of 4 lines with fixed T are close to each other, independently of the other parameters (t_d and γ_{th}). Inside each group, a little change arises when γ_{th} changes from 25 to 35 dB. This behavior may consequently lead to the investigation of a common classifier once T has been fixed. For example, the "average" line of each group may be used. This topic has been however left open for future research. To summarize, Bayes guarantees low error rates in a larger set of the parameters than the other techniques. More specifically, it is more reliable than the NN when $\gamma_{th} < 30$ dB.

V. Conclusions

This paper proposed novel feeder link outage prediction algorithms for possible use in future HTS systems operating in the EHF frequency bands. The use of the proposed prediction algorithms (LR, NN, and Bayes) showed significant improvement over traditional algorithms and opened the door to further developments in terms of adaptive prediction to non-stationary SNR.

Future extension of this work include the design of the full SDN-based network architecture, with the definition of QoS management solutions building on OpenFlow signaling.

References

[1] A. Kyrgiazos, B. Evans, and P. Thompson, "On the gateway diversity for high throughput broadband satellite systems," *Wireless Communications, IEEE Transactions on*, vol. 13, no. 10, pp. 5411–5426, Oct 2014.

[2] M. Muhammad, G. Giambene, and T. de Cola, "Channel prediction and network coding for smart gateway diversity in terabit satellite networks," in *Global Communications Conference (GLOBECOM), 2014 IEEE*, Dec 2014, pp. 3549–3554.

[3] I. R. Assembly, "Recommendation ITU-R P.1623-1 - Prediction Method of Fade Dynamics on Earth-Space Paths," Recommendation, International Telecommunication Union (ITU), Tech. Rep., Mar. 2005.

[4] L. Bertaux, S. Medjiah, P. Berthou, S. Abdellatif, A. Hakiri, P. Gelard, F. Planchou, and M. Bruyere, "Software defined networking and virtualization for broadband satellite networks," *Communications Magazine, IEEE*, vol. 53, no. 3, pp. 54–60, March 2015.

[5] "Digital video broadcasting (DVB); Second generation framing structure, channel coding and modulation systems for Broadcasting, Interactive Services, News Gathering and other broadband satellite applications (DVB-S2)," ETSI EN 302 307 V1.3.1, 2013.

[6] M. Casado, M. J. Freedman, J. Pettit, J. Luo, N. McKeown, and S. Shenker, "Ethane: Taking control of the enterprise," in *Proceedings of SIGCOMM '07*, 2007, pp. 1–12.

[7] N. McKeown, T. Anderson, H. Balakrishnan, G. Parulkar, L. Peterson, J. Rexford, S. Shenker, and J. Turner, "Openflow: Enabling innovation in campus networks," *SIGCOMM Comput. Commun. Rev.*, vol. 38, no. 2, pp. 69–74, Mar. 2008.

[8] L. Dossi, "Real-time prediction of attenuation for applications to fade countermeasures in satellite communications," *Electronics Letters*, vol. 26, no. 4, pp. 250–251, Feb 1990.

[9] A. Chambers and I. Otung, "Neural network approach to short-term fade prediction on satellite links," *Electronics Letters*, vol. 41, no. 23, pp. 1290–1292, Nov 2005.

[10] L. d. Montera, C. Mallet, L. Barthès, and P. Golé, "Short-term prediction of rain attenuation level and volatility in earth-to-satellite links at ehf band," *Nonlinear Processes in Geophysics*, vol. 15, no. 4, pp. 631–643, 2008.

[11] M. Luglio, "Fade prediction and control systems," in *Signals, Systems, and Electronics, 1995. ISSSE '95, Proceedings., 1995 URSI International Symposium on*, Oct 1995, pp. 71–75.

[12] B. Gremont, M. Filip, P. Gallois, and S. Bate, "Comparative analysis and performance of two predictive fade detection schemes for ka-band fade countermeasures," *Selected Areas in Communications, IEEE Journal on*, vol. 17, no. 2, pp. 180–192, Feb 1999.

[13] A. Gharanjik, B. Shankar, P.-D. Arapoglou, and B. Ottersten, "Multiple gateway transmit diversity in q/v band feeder links," *Communications, IEEE Transactions on*, vol. 63, no. 3, pp. 916–926, March 2015.

[14] S. Theodoridis and K. Koutroumbas, *Pattern Recognition, Fourth Edition*, 4th ed. Academic Press, 2008.

[15] L. Devroye, L. Györfi, and G. Lugosi, *A Probabilistic Theory of Pattern Recognition*. Springer, 1996.

[16] http://people.ku.edu/~gbohling/EECS833/Discrim.pdf.

[17] P. R. Gill, W. Murray, and M. H. Wright, *Practical Optimization*. Academic Press, 1981.